

SLIP EFFECTS ON UNSTEADY FREE CONVECTIVE HEAT AND MASS TRANSFER FLOW WITH NEWTONIAN HEATING

by

**Abid HUSSANAN^a, Ilyas KHAN^b, Mohd Z. SALLEH^a,
and Sharidan SHAFIE^{c*}**

^a Futures and Trends Research Group, Faculty of Industrial Science and Technology,
University Malaysia Pahang, Pahang, Malaysia

^b College of Engineering, Majmaah University, Majmaah, Saudi Arabia

^c Department of Mathematical Sciences, Faculty of Science,
University of Technology Malaysia, Skudai, Malaysia

Original scientific paper

DOI: 10.2298/TSCI131119142A

This article investigates the effects of slip condition on free convection flow of viscous incompressible fluid past an oscillating vertical plate with Newtonian heating and constant mass diffusion. The governing equations together with imposed initial and boundary conditions are solved using the Laplace transform technique. The results for velocity, temperature, and concentration are obtained and plotted for the embedded parameters. The results for skin friction, Nusselt number, and Sherwood number are computed in table. It is investigated that the presence of slip parameter reduces the fluid velocity.

Key words: slip effects, oscillating plate, Newtonian heating, heat transfer, mass transfer, Laplace transform

Introduction

The free convection flows together with heat and mass transfer are of great importance in geophysics, aeronautics, and engineering. In several process such as drying, evaporation of water at body surface, energy transfer in a wet cooling tower, and flow in a desert cooler, heat and mass transfer occurs simultaneously. Soundalgekar *et al.* [1, 2] for instance, have studied the mass transfer effects on the flow past an oscillating vertical plate with constant heat flux and variable temperature, respectively. Asogwa *et al.* [3] investigated heat and mass transfer past a vertical plate with periodic suction, and heat sink using perturbation technique. In addition, the interest of researchers to study the interaction of convection phenomenon with thermal radiation has been increased greatly during the last few decades due to its importance in many practical involvements. The advancement of space technology and in processes involving high thermal radiation effects play an important role. Recent developments in industrial technology have focused attention on thermal radiation as a mode of energy transfer, and emphasize the need for improved understanding of radiative transfer in these processes [4-6]. Radiation effects on free convection flow over a vertical plate with mass transfer were presented by Chamkha *et al.* [7]. Chandrakala and Bhaskar [8] also considered the radiation effects with uniform heat flux and mass diffusion. Recently, Abid *et al.* [9] stud-

* Corresponding author; e-mail: sharidan@utm.my

ied the MHD free convection flow with Newtonian heating condition in the presence of radiation and porosity effects.

Usually, the problems of free convection flows are modeled under the assumptions of constant surface temperature, ramped wall temperature or constant surface heat flux [10-12]. However, in many practical situations where the heat transfer from the surface is taken to be proportional to the local surface temperature, the previous assumptions fail to work. Such type of flows are termed as conjugate convective flows and the proportionally condition of the heat transfer to the local surface temperature is termed as Newtonian heating. This work was pioneered by Merkin [13] for the free convection boundary layer flow over a vertical flat plate immersed in a viscous fluid. However, due to numerous practical applications in many important engineering devices, several other researchers are getting interested to consider the Newtonian heating condition in their problems. Few of these applications are found in heat exchanger, heat management in electrical appliances (such as computer power supplies or substation transformer), and engine cooling (such as thin fins in car radiator). Literature survey shows that much attention to the problems of free convection flow with Newtonian heating is given by numerical solvers, as we can see [14-17], and the references therein. However, the exact solutions of these problems are very few [18-23].

In all these studies, the concept of slip condition is not taken into account. Recent interest in the study of vibrating flow with slip condition has been mainly motivated by its importance in microchannels or nanochannels. It is also known that slip can occur if the working fluid contains concentrated suspensions [24]. Seddeek and Abdelmeguid [25] studied effects of slip condition on magneto-micropolar fluid with combined forced and free convection in boundary layer flow over a horizontal plate. Under the influence of slip effects, Hayat *et al.* [26] studied oscillatory flow in a porous medium. In the same year, Hamza *et al.* [27] investigated the problem of unsteady heat transfer of an oscillatory flow through a porous medium under the slip boundary condition. Farhad *et al.* [28] analysed the influence of slip condition on unsteady MHD flow of Newtonian fluid induced by an accelerated plate. Recently, in another paper, Farhad *et al.* [29] developed exact solution for the hydromagnetic rotating flow of viscous fluid through a porous space under the influence of slip condition and Hall current. To the best of authors' knowledge, so far no study has been reported in the literature which investigates the slip effects on unsteady free convection flow of an incompressible viscous fluid past an oscillating vertical plate with Newtonian heating and constant mass diffusion. The present study is an attempt in this direction to fill this space.

Mathematical formulation

Let us consider unsteady free convection flow of an incompressible viscous fluid past an oscillating vertical plate with Newtonian heating and constant mass diffusion. The flow is assumed to be in the x' -direction which is taken along the plate in the vertical upward direction and the y' -axis is chosen normal to the plate. As the plate is considered infinite in x' -axis, therefore all physical variables are independent of x' and are functions of y' and t' . Initially, for time $t' \leq 0$, both the plate and fluid are at stationary condition with the constant temperature T_∞ and concentration C_∞ . After time $t' > 0$, the plate starts oscillatory motion in its plane with the velocity, $U_0 \cos(\omega t')$, against the gravitational field. At the same time, the heat transfer from the plate to the fluid is proportional to the local surface temperature, T' , and the concentration level near the plate is raised from C_∞ to C_w . Under the Boussinesq approximation, the flow is governed by the following partial differential equations [21, 23]:

$$\frac{\partial u'}{\partial t'} = \nu \frac{\partial^2 u'}{\partial y'^2} + g\beta(T' - T_\infty) + g\beta^*(C' - C_\infty) \quad (1)$$

$$\rho c_p \frac{\partial T'}{\partial t'} = k \frac{\partial^2 T'}{\partial y'^2} - \frac{\partial q_r}{\partial y'} \quad (2)$$

$$\frac{\partial C'}{\partial t'} = D \frac{\partial^2 C'}{\partial y'^2} \quad (3)$$

The initial and boundary conditions are:

$$t' \leq 0 : u' = 0, \quad T' = T_\infty, \quad C' = C_\infty \quad \text{for all } y' \geq 0 \quad (4)$$

$$t' > 0 : u' - \lambda \frac{\partial u'}{\partial y'} = U_0 \cos(\omega' t'), \quad \frac{\partial T'}{\partial y'} = -h_s T', \quad C' = C_w \quad \text{at } y' = 0, \quad (5)$$

$$u' \rightarrow 0, \quad T' \rightarrow T_\infty, \quad C' \rightarrow C_\infty \quad \text{as } y' \rightarrow \infty \quad (6)$$

The radiation heat flux under Rosseland approximation [30] is given by:

$$q_r = -\frac{4\sigma^*}{3k^*} \frac{\partial T'^4}{\partial y'} \quad (7)$$

It is also assumed that the difference between fluid temperature, T' , and ambient temperature, T_∞ , is sufficiently small so that T'^4 may be expressed as a linear function of the temperature. Expanding T'^4 in a Taylor series about T_∞ which after neglecting the second and higher order terms takes the form:

$$T'^4 \cong 4T_\infty^3 T' - 3T_\infty^4 \quad (8)$$

In view of eqs. (7) and (8), eq. (2) reduces to:

$$\rho c_p \frac{\partial T'}{\partial t'} = k \left(1 + \frac{16\sigma^* T_\infty^3}{3kk^*} \right) \frac{\partial^2 T'}{\partial y'^2} \quad (9)$$

To reduce the previous equations into their non-dimensional forms, we introduce the following non-dimensional quantities:

$$y = \frac{y' U_0}{\nu}, \quad t = \frac{t' U_0^2}{\nu}, \quad u = \frac{u'}{U_0}, \quad \theta = \frac{T' - T_\infty}{T_\infty}, \quad C = \frac{C' - C_\infty}{C_w - C_\infty}, \quad \omega = \frac{\omega' \nu}{U_0^2} \quad (10)$$

Substituting eq. (10) into eqs. (1), (3), and (9), we obtain the following non-dimensional partial differential equation:

$$\frac{\partial u}{\partial t} = \frac{\partial^2 u}{\partial y^2} + \text{Gr } \theta + \text{Gm } C \quad (11)$$

$$\text{Pr} \frac{\partial \theta}{\partial t} = (1 + R) \frac{\partial^2 \theta}{\partial y^2} \quad (12)$$

$$\text{Sc} \frac{\partial C}{\partial t} = \frac{\partial^2 C}{\partial y^2} \quad (13)$$

The corresponding initial and boundary conditions in non-dimensional forms are:

$$t \leq 0 : u = 0, \quad \theta = 0, \quad C = 0 \quad \text{for all } y \geq 0 \quad (14)$$

$$t > 0 : u - \gamma_1 \frac{\partial u}{\partial y} = \cos(\omega t), \quad \frac{\partial \theta}{\partial y} = -\gamma(1 + \theta), \quad C = 1 \quad \text{at } y = 0 \quad (15)$$

$$u \rightarrow 0, \quad \theta \rightarrow 0, \quad C \rightarrow 0 \quad \text{as } y \rightarrow \infty \quad (16)$$

where

$$\text{Gr} = \frac{\nu g \beta T_\infty}{U_0^3}, \quad \text{Gm} = \frac{\nu g \beta^* (C_w - C_\infty)}{U_0^3}, \quad \text{Pr} = \frac{\mu c_p}{k}$$

$$R = \frac{16 \sigma^* T_\infty^3}{3 k k^*}, \quad \text{Sc} = \frac{\nu}{D}, \quad \gamma_1 = \frac{\lambda U_0}{\nu}, \quad \gamma = \frac{h_s \nu}{U_0}$$

Method of solution

In order to obtain the exact solution of the present problem given by eqs. (11)-(16), we use the Laplace transform technique and obtain:

$$\begin{aligned} \bar{u}(y, q) = & \frac{c}{2} \left[\frac{1}{(q + i\omega)(\sqrt{q} + c)} e^{-y\sqrt{q}} \right] + \frac{c}{2} \left[\frac{1}{(q - i\omega)(\sqrt{q} + c)} e^{-y\sqrt{q}} \right] + \\ & + bc \left[\frac{1}{q^2 (\sqrt{q} + c)} e^{-y\sqrt{q}} \right] + ad \sqrt{\text{Pr}_{\text{eff}}} \left[\frac{\sqrt{q}}{q^2 (\sqrt{q} + c)(\sqrt{q} - d)} e^{-y\sqrt{q}} \right] + \\ & + b\sqrt{\text{Sc}} \left[\frac{\sqrt{q}}{q^2 (\sqrt{q} + c)} e^{-y\sqrt{q}} \right] + acd \left[\frac{1}{q^2 (\sqrt{q} + c)(\sqrt{q} - d)} e^{-y\sqrt{q}} \right] - \\ & - ad \left[\frac{1}{q^2 (\sqrt{q} - d)} e^{-y\sqrt{q} \text{Pr}_{\text{eff}}} \right] - b \left(\frac{1}{q^2} e^{-y\sqrt{q} \text{Sc}} \right) \end{aligned} \quad (17)$$

$$\bar{\theta}(y, q) = \frac{d}{q(\sqrt{q} - d)} e^{-y\sqrt{q} \text{Pr}_{\text{eff}}} \quad (18)$$

$$\bar{C}(y, q) = \frac{1}{q} e^{-y\sqrt{q} \text{Sc}} \quad (19)$$

where

$$a = \frac{Gr}{Pr_{\text{eff}} - 1}, \quad b = \frac{Gm}{Sc - 1}, \quad c = \frac{1}{\gamma_1}, \quad d = \frac{\gamma}{\sqrt{Pr_{\text{eff}}}}, \quad \text{and } Pr_{\text{eff}} = \frac{Pr}{1 + R}$$

is the effective Prandtl number defined by Magyari and Pantokratoras [30]. The inverse Laplace transform of eqs. (17)-(19) yields:

$$C(y, t) = F_1(\sqrt{Sc}y, t) \quad (20)$$

$$\theta(y, t) = F_4(\sqrt{Pr_{\text{eff}}}y, t, -d) - F_1(\sqrt{Pr_{\text{eff}}}y, t) \quad (21)$$

$$\begin{aligned} u(y, t) = & \alpha_1 F_5(y, t, -d) - \alpha_2 F_2(y, t) + \alpha_3 F_1(y, t) + \alpha_4 F_5(y, t, c) - \alpha_5 F_5(y, t, 0) + \\ & + \frac{a}{d} \left[F_2(\sqrt{Pr_{\text{eff}}}y, t) - F_2(y, t) \right] + \frac{a}{d^2} \left[F_1(\sqrt{Pr_{\text{eff}}}y, t) - F_1(y, t) \right] + \\ & + \frac{a}{d^3} \left[F_5(\sqrt{Pr_{\text{eff}}}y, t, 0) - F_5(\sqrt{Pr_{\text{eff}}}y, t, -d) - F_5(y, t, 0) \right] + \\ & + a \left[F_3(\sqrt{Pr_{\text{eff}}}y, t) - F_3(y, t) \right] - b \left[F_3(\sqrt{Sc}y, t) - F_3(y, t) \right] + \\ & + \alpha_{10} \left[cF_6(y, t, -i\omega) - \sqrt{-i\omega}F_7(y, t, -i\omega) \right] + \alpha_{11} \left[cF_6(y, t, i\omega) - \sqrt{i\omega}F_7(y, t, i\omega) \right] \quad (22) \end{aligned}$$

Note that the previous solutions are valid only for $\gamma_1 \neq 0$ and $Sc \neq 1$. Few other possible solutions are:

– *Case 1.* When $\gamma_1 \neq 0$ and $Sc = 1$:

$$\begin{aligned} u(y, t) = & \alpha_1 F_5(y, t, -d) - \alpha_6 F_2(y, t) + \alpha_7 F_1(y, t) + \alpha_8 F_5(y, t, c) - \alpha_9 F_5(y, t, 0) + \\ & + \frac{a}{d} \left[F_2(\sqrt{Pr_{\text{eff}}}y, t) - F_2(y, t) \right] + \frac{a}{d^2} \left[F_1(\sqrt{Pr_{\text{eff}}}y, t) - F_1(y, t) \right] + \\ & + \frac{a}{d^3} \left[F_5(\sqrt{Pr_{\text{eff}}}y, t, 0) - F_5(\sqrt{Pr_{\text{eff}}}y, t, -d) - F_5(y, t, 0) \right] + \\ & + a \left[F_3(\sqrt{Pr_{\text{eff}}}y, t) - F_3(y, t) \right] + \alpha_{10} \left[cF_6(y, t, -i\omega) - \sqrt{-i\omega}F_7(y, t, -i\omega) \right] + \\ & + \alpha_{11} \left[cF_6(y, t, i\omega) - \sqrt{i\omega}F_7(y, t, i\omega) \right] \quad (23) \end{aligned}$$

– *Case 2.* When $\gamma_1 = 0$ and $Sc \neq 1$:

$$\begin{aligned} u(y, t) = & \frac{1}{2} \left[F_6(y, t, -i\omega) + F_6(y, t, i\omega) \right] + \frac{a}{d} \left[F_2(\sqrt{Pr_{\text{eff}}}y, t) - F_2(y, t) \right] + \\ & + \frac{a}{d^2} \left[F_1(\sqrt{Pr_{\text{eff}}}y, t) - F_1(y, t) - F_4(\sqrt{Pr_{\text{eff}}}y, t, -d) + F_4(y, t, -d) \right] + \\ & + a \left[F_3(\sqrt{Pr_{\text{eff}}}y, t) - F_3(y, t) \right] - b \left[F_3(\sqrt{Sc}y, t) - F_3(y, t) \right] \quad (24) \end{aligned}$$

– Case 3. When $\gamma_1 = 0$ and $Sc = 1$:

$$\begin{aligned}
 u(y, t) = & \frac{1}{2} [F_6(y, t, -i\omega) + F_6(y, t, i\omega)] + \frac{a}{d} [F_2(\sqrt{\text{Pr}_{\text{eff}}} y, t) - F_2(y, t)] + \\
 & + \frac{a}{d^2} [F_1(\sqrt{\text{Pr}_{\text{eff}}} y, t) - F_1(y, t) - F_4(\sqrt{\text{Pr}_{\text{eff}}} y, t, -d) + F_4(y, t, -d)] + \\
 & + a [F_3(\sqrt{\text{Pr}_{\text{eff}}} y, t) - F_3(y, t)] + \frac{\text{Gm} y}{2} F_2(y, t) \quad (25)
 \end{aligned}$$

Here:

$$\begin{aligned}
 F_1(v, t) &= \text{erfc} \frac{v}{2\sqrt{t}}, & F_2(v, t) &= 2\sqrt{\frac{t}{\pi}} e^{-\frac{v^2}{4t}} - \text{verfc} \frac{v}{2\sqrt{t}}, \\
 F_3(v, t) &= \left(\frac{v^2}{2} + t\right) \text{erfc} \frac{v}{2\sqrt{t}} - v\sqrt{\frac{t}{\pi}} e^{-\frac{v^2}{4t}}, & F_4(v, t, \alpha) &= e^{(\alpha^2 t + \alpha v)} \text{erfc} \left(\frac{v}{2\sqrt{t}} + \alpha\sqrt{t}\right), \\
 F_5(v, t, \alpha) &= \frac{1}{\sqrt{\pi t}} e^{-\frac{v^2}{4t}} - \alpha e^{(\alpha^2 t + \alpha v)} \text{erfc} \left(\frac{v}{2\sqrt{t}} + \alpha\sqrt{t}\right), \\
 F_6(v, t, \alpha) &= \frac{1}{2} e^{\alpha t} \left[e^{-\sqrt{\alpha} v} \text{erfc} \left(\frac{v}{2\sqrt{t}} - \sqrt{\alpha t}\right) + e^{\sqrt{\alpha} v} \text{erfc} \left(\frac{v}{2\sqrt{t}} + \sqrt{\alpha t}\right) \right], \\
 F_7(v, t, \alpha) &= \frac{1}{2} e^{\alpha t} \left[e^{-\sqrt{\alpha} v} \text{erfc} \left(\frac{v}{2\sqrt{t}} - \sqrt{\alpha t}\right) - e^{\sqrt{\alpha} v} \text{erfc} \left(\frac{v}{2\sqrt{t}} + \sqrt{\alpha t}\right) \right], \\
 \alpha_1 &= \frac{a}{d^3(c+d)} (c + d\sqrt{\text{Pr}_{\text{eff}}}), & \alpha_2 &= \frac{a}{c} (\sqrt{\text{Pr}_{\text{eff}}} - 1) - \frac{b}{c} (\sqrt{Sc} - 1), \\
 \alpha_3 &= \frac{a}{c} \left(\frac{1}{c} - \frac{1}{d}\right) (\sqrt{\text{Pr}_{\text{eff}}} - 1) - \frac{b}{c^2} (\sqrt{Sc} - 1), \\
 \alpha_4 &= \frac{c^3}{c^4 + \omega^2} + \frac{ad}{c^3(c+d)} (\sqrt{\text{Pr}_{\text{eff}}} - 1) - \frac{b}{c^3} (\sqrt{Sc} - 1), \\
 \alpha_5 &= \frac{c^3}{c^4 + \omega^2} + \frac{a}{c} \left(\frac{1}{c^2} + \frac{1}{d^2} - \frac{1}{cd}\right) (\sqrt{\text{Pr}_{\text{eff}}} - 1) - \frac{b}{c^3} (\sqrt{Sc} - 1), \\
 \alpha_6 &= \frac{a}{c} (\sqrt{\text{Pr}_{\text{eff}}} - 1) - \frac{\text{Gm}}{2} - \frac{\text{Gm} y}{2}, & \alpha_7 &= \frac{a}{c} \left(\frac{1}{c} - \frac{1}{d}\right) (\sqrt{\text{Pr}_{\text{eff}}} - 1) - \frac{\text{Gm}}{2c}, \\
 \alpha_8 &= \frac{c^3}{c^4 + \omega^2} + \frac{ad}{c^3(c+d)} (\sqrt{\text{Pr}_{\text{eff}}} - 1) - \frac{\text{Gm}}{2c^2}, \\
 \alpha_9 &= \frac{c^3}{c^4 + \omega^2} + \frac{a}{c} \left(\frac{1}{c^2} + \frac{1}{d^2} - \frac{1}{cd}\right) (\sqrt{\text{Pr}_{\text{eff}}} - 1) - \frac{\text{Gm}}{2c^2}, \\
 \alpha_{10} &= \frac{c}{2(c^2 + i\omega)}, & \alpha_{11} &= \frac{c}{2(c^2 - i\omega)}
 \end{aligned}$$

where v and α are dummy variable and

$$\operatorname{erfc}(x) = 1 - \operatorname{erf}(x) = \frac{2}{\sqrt{\pi}} \int_0^x e^{-\eta^2} d\eta$$

The dimensionless expression of skin friction is given by:

$$\begin{aligned} \tau &= \frac{\nu \tau'}{\mu U_0^2} = - \frac{\partial u}{\partial y} \Big|_{y=0}, \\ \tau &= \frac{1}{\sqrt{\pi t}} \left[c(\alpha_{12} + \alpha_{13} - \alpha_1) - 2\alpha_{11} \sqrt{\operatorname{Sc}t} + d\alpha_2 + \alpha_3 \sqrt{\pi t} - \alpha_5 + 2\alpha_6 t \right] + \\ &\quad + \frac{1}{\sqrt{\pi t}} \left[\sqrt{\operatorname{Pr}_{\text{eff}}} \left(\alpha_{10} - d\alpha_7 + 2\alpha_8 t + \alpha_9 \sqrt{\pi t} \right) \right] + \\ &\quad + c\alpha_{12} \sqrt{-i\omega} e^{-i\omega t} \left[1 - \operatorname{erfc} \left(\sqrt{-i\omega t} \right) \right] + c\alpha_{13} \sqrt{i\omega} e^{i\omega t} \left[1 - \operatorname{erfc} \left(\sqrt{i\omega t} \right) \right] + \\ &\quad + \alpha_1 c^2 e^{c^2 t} \operatorname{erfc} \left(c\sqrt{t} \right) - \alpha_2 d^2 e^{d^2 t} \operatorname{erfc} \left(d\sqrt{t} \right) + \alpha_7 \sqrt{\operatorname{Pr}_{\text{eff}}} d^2 e^{d^2 t} \operatorname{erfc} \left(d\sqrt{t} \right) + \\ &\quad + i\omega \left(\alpha_{12} e^{-i\omega t} - \alpha_{13} e^{i\omega t} \right) + 2d^2 e^{d^2 t} \left(\alpha_{10} - \alpha_7 \sqrt{\operatorname{Pr}_{\text{eff}}} \right) \end{aligned} \quad (26)$$

Similarly for Nusselt and Sherwood numbers we write:

$$\operatorname{Nu} = - \frac{\nu}{U_0(T - T_\infty)} \frac{\partial T'}{\partial y'} \Big|_{y'=0} = \frac{1}{\theta(0, t)} + 1, \quad \operatorname{Nu} = d\sqrt{\operatorname{Pr}_{\text{eff}}} \left(1 + \frac{1}{e^{d^2 t} \left[1 + \operatorname{erf} \left(d\sqrt{t} \right) \right] - 1} \right) \quad (27)$$

$$\operatorname{Sh} = - \frac{\partial C}{\partial y} \Big|_{y=0} = \sqrt{\frac{\operatorname{Sc}}{\pi t}} \quad (28)$$

Graphical results and discussion

We have solved the problem of unsteady free convection flow of viscous incompressible fluid past an oscillating plate with Newtonian heating and constant mass diffusion in the presence of slip effects. Now it is important to study the effects of all parameters involved in the problem such as Prandtl number, radiation parameter, R , Grashof number, modified Grashof number, G_m , Schmidt number, dimensionless slip parameter, γ_1 , Newtonian heating parameter, γ , time, t , and phase angle, ωt . Numerical results for velocity, temperature, and concentration are graphically shown in figs. 1-16, whereas results for skin friction, Nusselt and Sherwood numbers are shown in tab. 1.

The effect of Prandtl number on the velocity field is shown in fig. 1. Four physical values of the Prandtl number, $\operatorname{Pr} = 0.71$ (air), $\operatorname{Pr} = 1.0$ (electrolytic solution), $\operatorname{Pr} = 7.0$ (water), and $\operatorname{Pr} = 100$ (engine oil), are chosen. It is observed that velocity decreases with increasing Prandtl number. Physically, it meets the logic that fluids with large Prandtl number have high viscosity and small thermal conductivity, which makes the fluid thick, and hence causes a decrease in the velocity of the fluid. The effect of the radiation parameter, R , on the velocity field is shown in fig. 2. It is observed that velocity increases for large values of the radiation parameter. Such a variation in velocity with R is physically acceptable because higher radiation occurs when temperature is high and eventually velocity rises. This figure also

Table 1. Numerical results for skin friction, Nusselt and Sherwood number

| t | R | Pr | Gr | Gm | Sc | γ | γ_1 | ωt | τ | Nu | Sh |
|-----|-----|------|------|------|------|----------|------------|------------|--------|--------|--------|
| 0.1 | 0.5 | 1 | 3 | 2 | 0.22 | 1 | 0.5 | $\pi/2$ | 0.7140 | 2.5496 | 0.8368 |
| 0.2 | 0.5 | 1 | 3 | 2 | 0.22 | 1 | 0.5 | $\pi/2$ | 0.0752 | 1.9027 | 0.5917 |
| 0.1 | 1.0 | 1 | 3 | 2 | 0.22 | 1 | 0.5 | $\pi/2$ | 0.6288 | 2.2515 | – |
| 0.1 | 0.5 | 7 | 3 | 2 | 0.22 | 1 | 0.5 | $\pi/2$ | 0.9231 | 6.8785 | – |
| 0.1 | 0.5 | 1 | 5 | 2 | 0.22 | 1 | 0.5 | $\pi/2$ | 0.6538 | – | – |
| 0.1 | 0.5 | 1 | 3 | 4 | 0.22 | 1 | 0.5 | $\pi/2$ | 0.5321 | – | – |
| 0.1 | 0.5 | 1 | 3 | 2 | 0.62 | 1 | 0.5 | $\pi/2$ | 0.7464 | – | 1.4048 |
| 0.1 | 0.5 | 1 | 3 | 2 | 0.22 | 2 | 0.5 | $\pi/2$ | 0.5403 | 2.9318 | – |
| 0.1 | 0.5 | 1 | 3 | 2 | 0.22 | 1 | 1.0 | $\pi/2$ | 0.4885 | – | – |
| 0.1 | 0.5 | 1 | 3 | 2 | 0.22 | 1 | 0.5 | π | 0.5016 | – | – |

shows the comparison of pure convection ($R = 0$) and radiation. It is found that in case of pure convection the velocity is minimum.

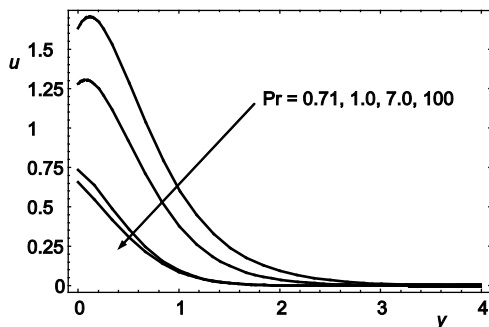


Figure 1. Velocity profiles for different values of Pr , when $t = 0.2$, $R = 3$, $Gr = 5$, $Gm = 2$, $Sc = 0.78$, $\gamma_1 = 0.5$, $\gamma = 1$, and $\omega = \pi/2$

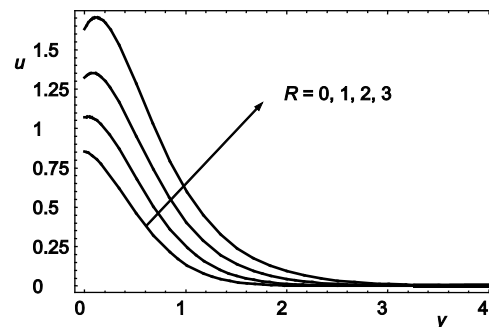


Figure 2. Velocity profiles for different values of R , when $t = 0.2$, $Gr = 5$, $Gm = 2$, $Pr = 0.71$, $Sc = 0.78$, $\gamma_1 = 0.5$, $\gamma = 1$, and $\omega = \pi/2$

Grashof number, is the characteristic dimensionless group which approximates the ratio of the buoyancy to viscous force acting on a fluid. It frequently arises in the study of situations involving natural convection. The influence of Grashof number on velocity profiles is shown in fig. 3. It is found that the velocity profiles increase with increasing values of Grashof number. Physically, it is due to the fact that as we increase Grashof number it gives rise to the thermal buoyancy effects which gives rise to an increase in the induced flow. On the other hand, the modified Grashof number, Gm , is found to have similar effects on velocity profiles as observed for the Grashof number. This fact is shown in fig. 4. Further, from these figures (figs. 3 and 4), it is noticed that Grashof number and modified Grashof number do not have any influence as the fluid move away from the bounding surface.

The velocity profiles for different values of Schmidt number, are shown in fig. 5. Four different values of Schmidt number, $Sc = 0.22$, 0.62 , 0.78 , and 0.94 , are chosen. They physically correspond to hydrogen, water vapour, ammonia, and CO_2 , respectively. It is clear

that the velocity decreases as the Schmidt number increases. Further, it is clear from this figure that velocity for hydrogen is maximum and CO₂ carries the minimum velocity. Further, the effects of slip parameter, γ_1 , on the velocity field are shown in fig. 6. It is observed from this figure that velocity decreases with increasing values of γ_1 . Note that the variations in velocity due to slip parameter are identical to the published work of Farhad *et al.* [28, 29], see figs. 1 and 7(a). The velocity profiles for different values of the Newtonian heating parameter,

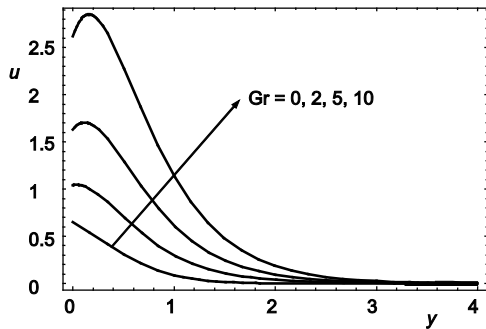


Figure 3. Velocity profiles for different values of Gr, when $t = 0.2$, $R = 3$, $Gm = 2$, $Pr = 0.71$, $Sc = 0.78$, $\gamma_1 = 0.5$, $\gamma = 1$, and $\omega = \pi/2$

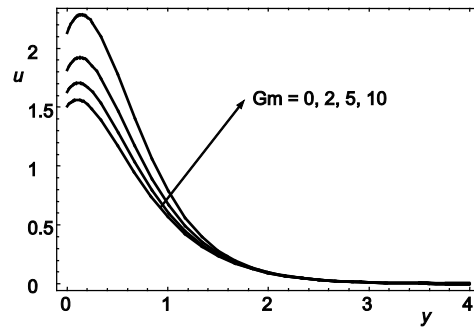


Figure 4. Velocity profiles for different values of Gm, when $t = 0.2$, $R = 3$, $Gr = 5$, $Pr = 0.71$, $Sc = 0.78$, $\gamma_1 = 0.5$, $\gamma = 1$, and $\omega = \pi/2$

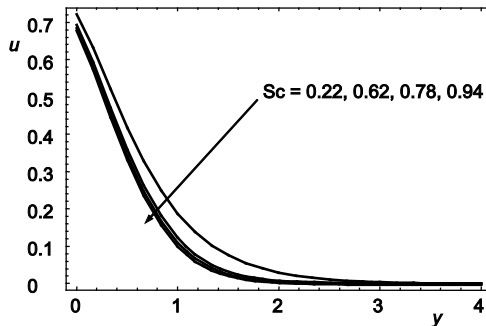


Figure 5. Velocity profiles for different values of Sc, when $t = 0.2$, $R = 3$, $Gr = 5$, $Pr = 0.71$, $Gm = 2$, $\gamma_1 = 1$, $\gamma = 0.1$, and $\omega = \pi/2$

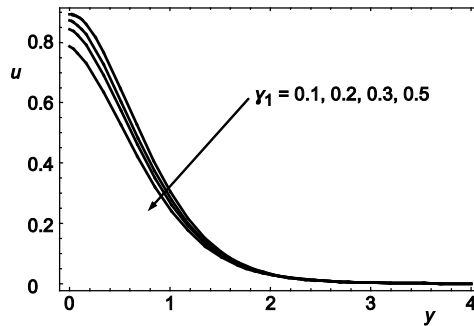


Figure 6. Velocity profiles for different values of γ_1 , when $t = 0.2$, $R = 3$, $Gr = 5$, $Gm = 2$, $Pr = 0.71$, $Sc = 0.78$, $\gamma = 1$, and $\omega = \pi/2$

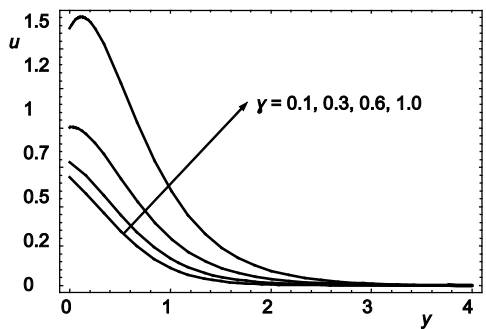


Figure 7. Velocity profiles for different values of γ , when $t = 0.2$, $R = 3$, $Gr = 5$, $Gm = 2$, $Pr = 0.71$, $Sc = 0.78$, $\gamma_1 = 1$, and $\omega = \pi/2$

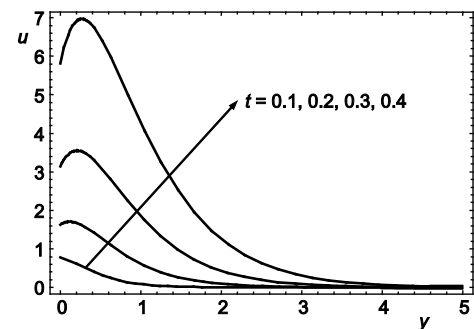


Figure 8. Velocity profiles for different values of t , when $R = 3$, $Gr = 5$, $Gm = 3$, $Pr = 0.71$, $Sc = 0.78$, $\gamma_1 = 0.5$, $\gamma = 1$, and $\omega = \pi/2$

γ , are presented in fig. 7. It is found that as the Newtonian heating parameter increases, the density of the fluid decreases and the momentum boundary layer thickness increases and as a result, the velocity increases within the boundary layer. Further, it is observed from fig. 8 that the fluid velocity increases with an increase in time, t . The velocity profiles for different values of phase angle, ωt , are shown in fig. 9. It is observed that velocity shows an oscillatory behavior. The velocity near the plate is maximum and decreasing with increasing distance from the plate, finally approaches to zero as $y \rightarrow \infty$. Further, the velocity profiles are shown in Fig. 10 for two different values of Schmidt number in the presence of slip parameter ($\gamma_1 \neq 0$), as well as in the absence of slip parameter ($\gamma_1 = 0$). It is found that in the absence of slip parameter when $Sc < 1$, the velocity has its maximum values. However, velocity is found to decrease when Schmidt number increases from 0.72 to 1. The velocity is further decreased in the presence of slip parameter for the unit value of the Schmidt number by keeping other parameters fixed.

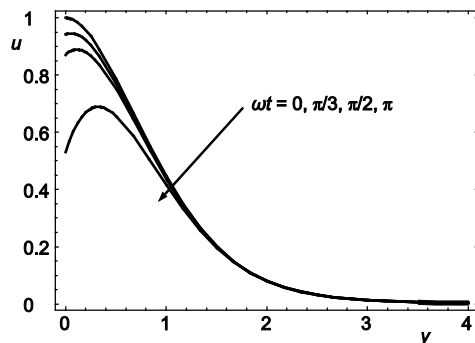


Figure 9. Velocity profiles for different values of ωt , when $t = 0.4$, $R = 3$, $Gr = 5$, $Gm = 2$, $Sc = 0.78$, $\gamma_1 = 0.5$ and $\gamma = 1$

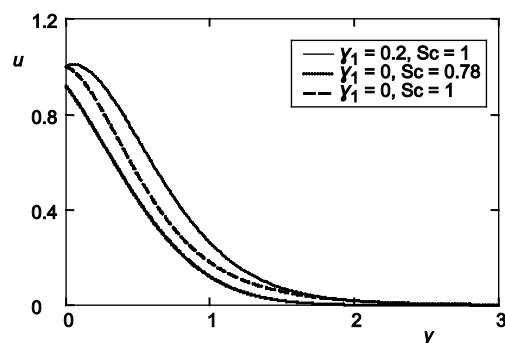


Figure 10. Velocity profiles for different values of γ_1 and Sc , when $t = 0.2$, $R = 3$, $Pr = 0.71$, $Gr = 5$, $Gm = 3$, $\gamma = 1$, and $\omega = 0$

On the other hand, the effects of Prandtl number on the temperature are shown in fig. 11. It is observed that the temperature decreases with the increase of Prandtl number. Physically, it is due to the fact that with increasing Prandtl number, thermal conductivity of fluid decreases and viscosity of the fluids increases and as a result the thermal boundary layer decreases with increasing Prandtl number. On the other hand, the buoyancy that results from the thermal expansion of fluid adjacent to the surface is the cause for the development of a rising boundary layer. Consequently, it is found from the comparison of figs. 1 and 11 that the velocity boundary layer is thicker than the thermal boundary layer because the buoyant fluid layer causes macroscopic motion in a thicker fluid layer due to the strong viscosity.

The effects of radiation parameter, R , on the temperature are shown in fig. 12, where $R = 0$ indicates to the case of no thermal radiation. It is observed that the temperature increases with an increasing R . Physically it is due to the fact that the job of thermal radiation is to increase the thermal boundary layer thickness. It is found from fig. 13 that the effects of time, t , on the temperature are quite identical to that on the velocity profiles. Further, it is found from fig. 14 that an increase in the Newtonian heating parameter increases the thermal boundary layer thickness and as a result the surface temperature of the plate increases. Finally, it is observed from all the temperature profiles that the temperature is maximum near the plate and decreases away from the plate and finally asymptotically approaches to zero in the free stream region. It is found from fig. 15 that the influence of time, t , on concentration profiles is similar

to velocity and temperature profiles given in figs. 8 and 13. The effects of Schmidt number on the concentration profiles are shown in fig. 16. It is seen from this figure that an increase in value of Schmidt number makes the concentration boundary layer thin and hence the concentration profiles decrease.

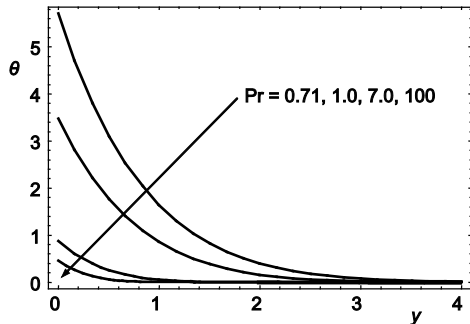


Figure 11. Temperature profiles for different values of Pr , when $t = 2$, $R = 5$, and $\gamma = 0.01$

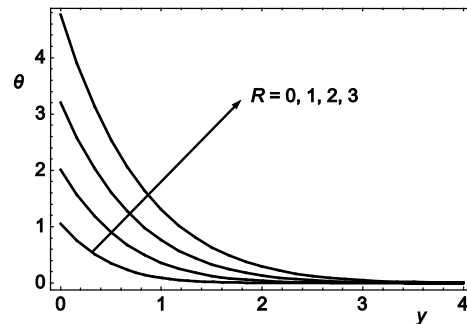


Figure 12. Temperature profiles for different values of R , when $t = 0.2$, $Pr = 0.71$, and $\gamma = 1$

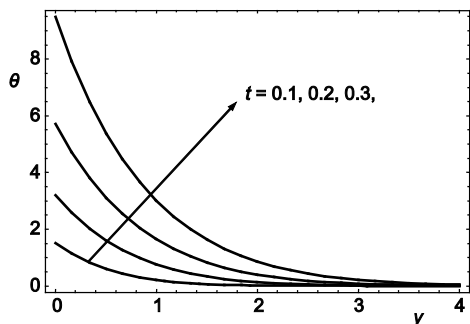


Figure 13. Temperature profiles for different values of t , when $R = 2$, $Pr = 0.71$, and $\gamma = 1$

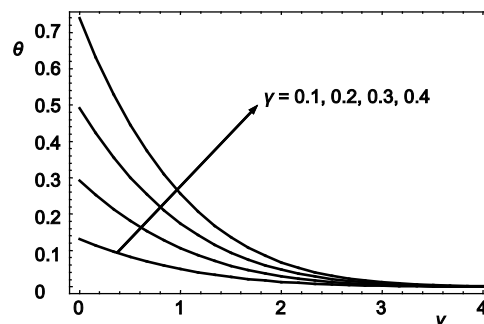


Figure 14. Temperature profiles for different values of γ , when $t = 0.2$, $R = 0.5$, and $Pr = 0.71$

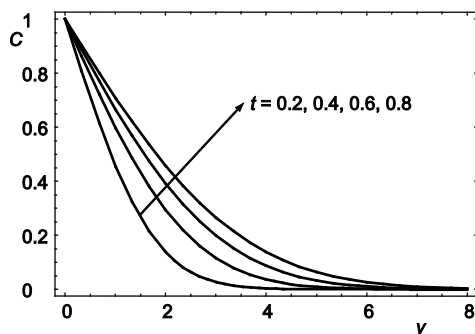


Figure 15. Concentration profiles for different values of t , when $Sc = 0.22$

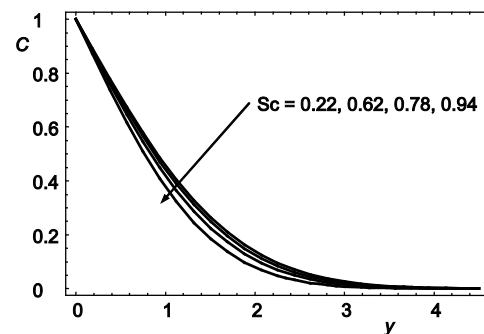


Figure 16. Concentration profiles for different values of Sc , when $t = 0.2$

The numerical results for skin friction, Nusselt and Sherwood numbers for different parameters are presented in tab. 1. It is found from this table that skin friction decreases with increasing values of radiation parameter, R , Grashof number, modified Grashof number, G_m , Newtonian heating parameter, γ , slip parameter, γ_1 , time, t , and phase angle, ωt , while it in-

creases as Prandtl and Schmidt numbers are increased. The Nusselt number is found to increase with increasing values of Prandtl number and Newtonian heating parameter, γ , but decreases when radiation R and t are increased. Further, it is observed that the Sherwood number increases with increasing Schmidt number, while reverse effect is observed for t .

Conclusion

The work considered here provides an exact analysis of unsteady free convective heat and mass transfer flow of a viscous incompressible past an oscillating vertical plate with Newtonian heating in the presence of radiation and slip effects. The results obtained show that the velocity increases with increasing values of the radiation parameter, Grashof number, modified Grashof number, Newtonian heating parameter, and time. However, the skin friction is decreased when these parameters are increased. The Nusselt number increases with the increasing values of Newtonian heating parameter as well as with Prandtl number. The Sherwood number decreases with increasing values of time but increases with increasing the values of Schmidt number. Moreover, the exact solutions obtained in this study are significant not only because they are solutions of some fundamental flows, but also serve as accuracy standards for approximate methods.

Acknowledgment

The authors would like to acknowledge MOHE and Research Management Centre-UTM for the financial support through vote numbers 4F255 and 04H27 for this research. The authors also gratefully acknowledge the financial supports received from the Universiti Malaysia Pahang, Malaysia through vote numbers RDU121302 and RDU131405 for this research.

Nomenclature

| | |
|--|---|
| C' – species concentration in the fluid [molm^{-3}] | u' – velocity of the fluid in the x' -direction [ms^{-1}] |
| C_∞ – species concentration in the fluid far away from the plate [molm^{-3}] | U_0 – amplitude of oscillation [m] |
| c_p – heat capacity at constant pressure [$\text{Jkg}^{-1}\text{K}^{-1}$] | <i>Greek symbols</i> |
| C_w – species concentration near the plate [molm^{-3}] | β – volumetric coefficient of thermal expansion [K^{-1}] |
| D – mass diffusivity [m^2s^{-1}] | β^* – volumetric coefficient of mass expansion [K^{-1}] |
| Gm – modified Grashof number | γ – Newtonian heating parameter |
| Gr – thermal Grashof number | γ_1 – dimensionless slip parameter |
| g – acceleration due to gravity [ms^{-2}] | θ – dimensionless temperature |
| h_s – heat transfer coefficient | λ – slip parameter |
| k – thermal conductivity [$\text{Wm}^{-1}\text{K}^{-1}$] | μ – dynamic viscosity, [$\text{kgm}^{-1}\text{s}^{-1}$] |
| k^* – mean absorption coefficient | ν – kinematic viscosity [m^2s^{-1}] |
| Pr – Prandtl number | ρ – fluid density [kgm^{-3}] |
| q – Laplace transform parameter | σ^* – Stefan-Boltzmann constant [$\text{Wm}^{-2}\text{K}^{-4}$] |
| q_r – radiative heat flux in the y' -direction [Wm^{-2}] | τ – dimensionless skin friction |
| R – radiation parameter | τ' – skin friction |
| Sc – Schmidt number | ω' – frequency of oscillation |
| T' – temperature of the fluid [K] | ωt – phase angle |
| T_∞ – ambient temperature [K] | |
| t' – dimensionless time [s] | |

References

- [1] Soundalgekar, V. M., et al., Effects of Mass Transfer on the Flow Past an Oscillating Infinite Vertical Plate with Constant Heat Flux, *Thermophysics and AeroMechanics*, 1 (1994), 2, pp. 119-124

- [2] Soundalgekar, V. M., et al., Mass Transfer Effects on Flow Past a Vertical Oscillating Plate with Variable Temperature, *Heat and Mass transfer*, 30 (1995), 5, pp. 309-312
- [3] Asogwa, K. K., et al., Heat and Mass Transfer over a Vertical Plate With Periodic Suction and Heat Sink, *Research Journal of Applied Sciences, Engineering and Technology*, 5 (2013), 1, pp. 7-15
- [4] Das, U. N., et al., Radiation Effects on Flow Past an Impulsively Started Vertical Infinite Plate, *Journal of Theoretical Mechanics*, 1 (1996), 5, pp. 111-115
- [5] Raptis, A., Perdikis, C., Radiation and Free Convection Flow past a Moving Plate, *International Journal of Applied Mechanics and Engineering*, 4 (1999), 4, pp. 817-821
- [6] Das, S., et al., Radiation Effect on Natural Convection Near a Vertical Plate Embedded in Porous Medium with Ramped Wall Temperature, *Open Journal of Fluid Dynamics*, 1 (2011), 1, pp. 1-11
- [7] Chamkha, A. J., et al., Radiation Effects on Free Convection Flow Past a Semi-Infinite Vertical Plate with Mass Transfer, *Chemical Engineering Journal*, 84 (2011), 3, pp. 335-342
- [8] Chandrakala, P., Bhaskar, P. N., Radiation Effects on Oscillating Vertical Plate with Uniform Heat Flux and Mass Diffusion, *International Journal of Fluids Engineering*, 4 (2012), 1, pp. 1-11
- [9] Abid, H., et al., Unsteady Boundary Layer MHD Free Convection Flow in a Porous Medium with Constant Mass Diffusion and Newtonian Heating, *European Physical Journal Plus*, 129 (2014), 3, pp. 1-16
- [10] Hossain, M. A., Takhar, H. S., Radiation Effect on Mixed Convection Along a Vertical Plate with Uniform Surface Temperature, *Heat and Mass Transfer*, 31 (1996), 4, pp. 243-248
- [11] Deka, R. K., Das, S. K., Radiation Effects on Free Convection Flow Near a Vertical Plate with Ramped Wall Temperature, *Engineering*, 3 (2011), 12, pp. 1197-1206
- [12] Chandrakala, P., Radiation Effects on Flow Past an Impulsively Started Vertical Oscillating Plate with Uniform Heat Flux, *International Journal of Dynamics of Fluid*, 6 (2010), 2, pp. 209-215
- [13] Merkin, J. H., Natural Convection Boundary Layer Flow on a Vertical Surface with Newtonian Heating, *International Journal of Heat and Fluid Flow*, 15 (1994), 5, pp. 392-398
- [14] Salleh, M. Z., et al., Boundary Layer Flow and Heat Transfer over a Stretching Sheet with Newtonian Heating, *Journal of the Taiwan Institute of Chemical Engineers*, 41 (2010), 6, pp. 651-655
- [15] Salleh, M. Z., et al., Forced Convection Heat Transfer over a Circular Cylinder with Newtonian Heating, *Journal of Engineering Mathematics*, 69 (2011), 1, pp. 101-110
- [16] Kasim, A. R. M., et al., Natural Convection Boundary Layer Flow of a Viscoelastic Fluid on Solid Sphere with Newtonian Heating, *World Academy of Science, Engineering and Technology*, 6 (2012), 4, pp. 410-415
- [17] Das, S., et al., Radiation Effects on Unsteady Free Convection Flow Past a Vertical Plate with Newtonian Heating, *International Journal of Computer Applications*, 41 (2012), 13, pp. 36-41
- [18] Chaudhary, R. C., Jain, P., Unsteady Free Convection Boundary Layer Flow Past an Impulsively Started Vertical Surface with Newtonian Heating, *Romanian Journal of Physics*, 51 (2006), 9-10, pp. 911-925
- [19] Mebine, P., Adigio, E. M., Unsteady Free Convection Flow with Thermal Radiation Past a Vertical Porous Plate with Newtonian Heating, *Turkish Journal of Physics*, 33 (2009), 2, pp. 109-119
- [20] Narahari, M., Ishak, A., Radiation Effects on Free Convection Flow Near a Moving Vertical Plate with Newtonian Heating, *Journal of Applied Sciences*, 11 (2011), 7, pp. 1096-1104
- [21] Narahari, M., Nayan, M. Y., Free Convection Flow Past an Impulsively Started Infinite Vertical Plate with Newtonian Heating in the Presence of Thermal Radiation and Mass Diffusion, *Turkish Journal of Engineering and Environmental Science*, 35 (2011), 3, pp. 187-198
- [22] Hussanan, A., et al., Natural Convection Flow Past an Oscillating Plate with Newtonian Heating, *Heat Transfer Research*, 45 (2014), 2, pp. 119-135
- [23] Hussanan, A., et al., An Exact Analysis of Heat and Mass Transfer Past a Vertical Plate with Newtonian Heating, *Journal of Applied Mathematics*, 2013 (2013), ID 434571
- [24] Soltani, F., Yilmazar, U., Slip Velocity and Slip Layer Thickness in Flow of Concentrated Suspensions, *Journal of Applied Polymer Science*, 70 (1998), 3, pp. 515-522
- [25] Seddeek, M. A., Abdelmeguid, M. S., Hall and Ion Slip Effects on Magneto-Micropolar Fluid with Combined Forced and Free Convection in Boundary Layer Flow over a Horizontal Plate, *Journal of the Korean Society for Industrial and Applied Mathematics*, 8 (2004), 2, pp. 51-73
- [26] Hayat, T., et al., Slip Effects on the Oscillatory Flow in a Porous Medium, *Journal of Porous Media*, 14 (2011), 6, pp. 481-493
- [27] Hamza, M. M., et al., Unsteady Heat Transfer to MHD Oscillatory Flow through a Porous Medium under Slip Condition, *International Journal of Computer Applications*, 33 (2011), 4, pp. 12-17

- [28] Farhad, A., et al., On Accelerated MHD Flow in a Porous Medium with Slip Condition, *European Journal of Scientific Research*, 57 (2011), 2, pp. 293-304
- [29] Farhad, A., et al., On Hydromagnetic Rotating Flow in a Porous Medium with Slip Condition and Hall Current, *International Journal of the Physical Sciences*, 7 (2011), 10, pp. 1540-1548
- [30] Magyari, E., Pantokratoras, A., Note on the Effect of Thermal Radiation in the Linearized Rosseland Approximation on the Heat Transfer Characteristics of Various Boundary Layer Flows, *International Communications in Heat and Mass Transfer*, 38 (2011), 5, pp. 554-556